Variable Speed Hydropower Conversion and Control

Tor Inge Reigstad, Kjetil Uhlen, *Member, IEEE*

***Abstract*—The objective of this paper is to develop and analyse a variable speed hydropower (VSHP) model that can aid the design of controllers that maximize the utilization of power plant for the provision of ancillary services, considering the limitations given by the hydraulic system. The model is tested and analysed with more or less conventional controllers to identify critical modes, adverse interactions or other limitations that must be taken into account in the future design of potentially multivariable or more advanced controllers for VSHP. Dynamic tests are performed by simulating step responses in power demand and by comparing responses of the model with the VSHP and with a conventional hydropower plant. A participation factor-based interaction analysis shows that there are no strong dynamic couplings between the hydraulic system of the VSHP and the rest of the grid. This simplifies the tuning of the control system. However, the analysis concludes that some oscillatory modes associated with the hydraulic system become significantly more excited when operating at variable speed; which is due to the larger deviation in turbine rotational speed. Extra awareness when designing the control system is therefore needed to keep the hydraulic system variables within their limits.**

***Index Terms*—AC-AC power conversion, eigenvalues and eigenfunctions, frequency control, hydraulic systems, hydraulic turbines, hydroelectric power generation, power generation control, power system modeling, power system simulation, stability.**

I. Introduction

MORE flexible resources are required to control the balance of the grid and to maintain the power system security as the share of electricity generation from variable renewables increases. Variable speed hydropower (VSHP) plants represent one solution that has the potential to contribute effectively to the required flexibility. The hypothesis is that VSHP plants can offer additional ancillary services by contributing more effectively to frequency control and this maintaining of grid stability, thus allowing for higher penetration of variable renewables in the grid. The advantage compared to conventional pumped-storage hydropower with constant rotational speed is more effective utilization of the kinetic energy in the turbine and generator and improved power control in pumping mode. The efficiency and operating range of VSHP will also be higher and they can contribute to frequency control both in the generation and in the pumping mode. [1] The converter technology offers faster control of reactive power and potentially higher reactive power capability, which benefits the voltage regulation. Compared with conventional hydropower plants, the VSHP enables a further degree of freedom to control power and speed. This opens new possibilities, but also necessitates proper co-ordination of the controls - and there will be new constraints that must be taken into account.

A detailed model of the VSHP system is needed to investigate the interactions between the VSHP plant and the grid, how variable speed operation can benefit the security and flexibility of the power system operation and to explore the control possibilities from a system perspective while considering the limitations given by the water/turbine system. This comprises the development of non-linear time-domain simulation models with limitations for water flows in the tunnel, turbine, governor, generator with a magnetizing system, generator-side converter and grid-side converter, and a representative test grid. This paper will focus on the converter models and the interaction between the hydraulic system in the VSHP and the grid.

A number of different dynamic models of VSHP including converter models have been presented in the last decade, most of which make use of doubly-fed induction generators (DFIG). There are large differences in the levels of detail in the models, especially in regard to hydraulic modelling. Reference [2] presents the modelling, simulation, and analysis of a VSHP with an electric equivalent hydraulic system, DFIG configuration and converter control system. In [3], a dynamic VSHP model including an elastic water column model, turbine model and DFIG is derived. An autonomous variable speed micro hydropower station with a simple Kaplan-model, DFIG configuration and converters is presented in [4]. Experimental results on a small VSHP with DFIG-configuration are shown in [5]. Dynamic modelling of adjustable-speed pumped storage hydropower plant with DFIG is performed in [6]. Reference [7] reviews technical considerations related to VSHP for the provision of frequency containment reserves (FCRs), and modelling and control for power system studies are discussed. Power regulation of VSHP for mitigating wind power variation is investigated in [8]. Reference [9] explores the improvement of power step performance for a VSHP compared to a conventional pumped storage power plant by using a numerical simulation model in SIMSEN. It is found that the maximum power step to the grid is strongly dependent on the hydro-mechanical characteristics of the power plant. In [10], four different hydraulic turbine models are compared to select a model that is best suited for use in grid integration studies of VSHP plants.

VSHP with a synchronous generator and full-power converters are found more rarely in the literature. A small VSHP with diode rectifier, DC-DC boost converter, optimal rotational speed control and converter control is presented in [11]. Reference [12] presents the dynamic modelling, simulation and control design of a small VSHP with diode rectifier, DC-DC boost converter, voltage source inverter and control

This work was supported by the Research Council of Norway under Grant 257588 and by the Norwegian Research Centre for Hydropower Technology (HydroCen).

T.I. Reigstad and K. Uhlen are with Department for Electric Power Engineering, Norwegian University of Science and Technology (NTNU), NO-7491 Trondheim, Norway (email: tor.inge.reigstad@ntnu.no, kjetil.uhlen@ntnu.no)

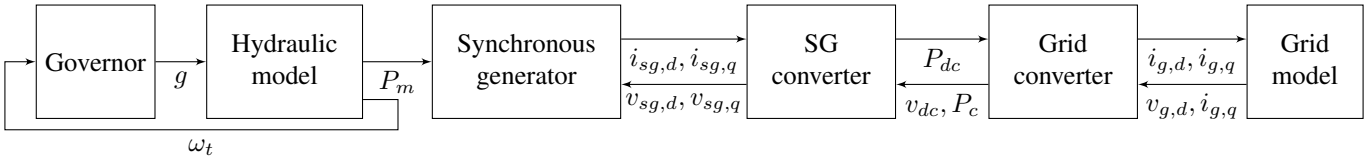

Fig. 1: Overview of VSHP model

system.

The main purpose of this paper is to present a complete model of a VSHP plant that can serve as a reference and basis for further development and choice of control systems. The paper is organized as follows: The variable speed hydropower models and the power system model are presented in Section II and III respectively. The dynamic analysis results and discussion are given in Section IV. Section V presents the theory, results and discussion from the participation factor analysis. Finally, in Section VI, the conclusions are given .

II. Variable Speed Hydropower Models

A. Control Objectives

A set of control objectives for a VSHP can be formulated as follows:

- Objectives for internal control of the plant:
  - Optimize the rotational speed of the turbine with respect to efficiency at part load.
  - Minimize water hammering and mass oscillations.
  - Minimize the guide vane servo operation.
  - Minimize the hydraulic and electric losses.
- Objectives for grid support control:
  - Contribute to the frequency containment reserves by faster and more precise frequency droop control.
  - Contribute to increasing the effective system inertia by virtual inertia (VI) control.
  - Improve the voltage control response time.

This paper will primarily concentrate on the internal control objectives. An overview of the VSHP with the variables connecting the subsystem is presented in Figure 1.

B. Hydraulic System Models

The hydraulic system is modelled with the Euler turbine equations model presented in [10]. The Euler turbine equations are used to describe how the hydraulic power is transformed into mechanical rotational power. The model presented in Figure 2 considers guide vane opening, pressure, water flow and rational speed. It is used together with a non-linear waterway model [13] to also consider travelling wave effects in the penstock (water hammer), headrace tunnel dynamics (mass oscillation), surge tank dynamics and head loss in the waterway. However, the model does not consider the effect of acceleration of the flow through the runner and the angular acceleration of the water masses in the runner [14]. The dimensionless turbine equations are derived in [14] where the dimensionless flow, head and angular speed of rotation are $q = Q/Q_R$, $h = H/H_R$ and $\tilde{\omega} = \omega/\omega_R$. Figure 3 shows the layout of the VSHP waterway and turbine.

C. Governor PID Controller without Permanent Droop

A governor with a PID controller and without permanent droop is chosen (1) for the VSHP. Droop control is not required since the shaft speed is decoupled from the grid and primary power-frequency control is performed by the grid converter. The PID controller output is saturated and rate limited.

$$\frac{g}{\Delta\omega} = \frac{g}{\omega^* - \omega} = \frac{k_{g,d}s^2 + k_{g,p}s + k_{g,i}}{s}\frac{1}{1 + T_G s} \tag{1}$$

III. Power System Model

A. Grid Model

The chosen basis for the grid model is the Two-Area Kundur grid model (Figure 4) as presented in Example 12.6b (iv) in [15], with the following changes:

- A *Hygov* governor is added to all generators in order to be able to compare the VSHP to conventional power plants.
- A 640 MW VSHP, as described below, is added at Bus5.

B. Grid Converter

The inner controller (4) of the grid converter, Figure 5, controls the d- and q-axis currents, while the outer controls the active power to the grid in the d-axis (2) and the reactive power to the grid in the q-axis (3). Alternatively, VI control can be implemented instead of standard active power control. The converter model, filter model and power calculation are given in (5) - (7) while the dc-link model is given in (8) and Figure 6. The parameters of the PI inner and outer controller are obtained by the Modulus Optimum (MO) and Symmetrical Optimum (SO) criterion, respectively, according to the approach explained in [16], [17], assuming a switching frequency of 1 kHz. The MO criterion is a simple and fast response tuning method for low order control plants without time delay and is used for tuning the inner loop. The method cancels the largest time constant, the filter constant, and ensures that the closed-loop gain is larger than one for as high frequencies as possible. The SO criterion is used to achieve maximum phase margin at the crossover frequency of the simplified outer loop, open-loop transfer function. A design parameter a is tuned to ensure that the bandwidth of the outer controller is approximately one decade below the bandwidth of the inner controller. The utilization of these methods ensures equivalent tuning of converters with different parameters and avoids the use of " trial and error" methods.

1) Outer Controller - Active Power Control:

$$\begin{aligned} \frac{d}{dt}N_{c,d} &= k_{Pi}\left(P_g^* - P_g\right) \\ i_{g,d}^* &= k_{Pp}\left(P_g^* - P_g\right) + N_{c,d} \end{aligned} \tag{2}$$

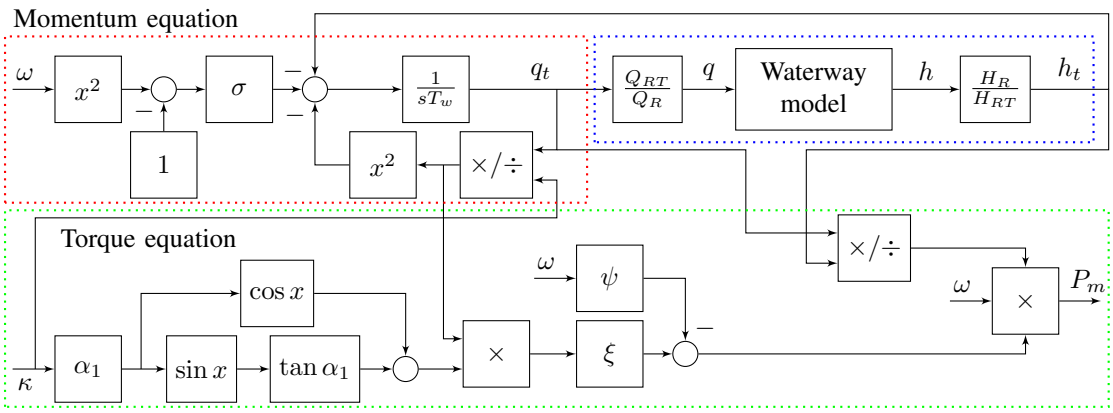

Fig. 2: Turbine model based on the Euler Equations

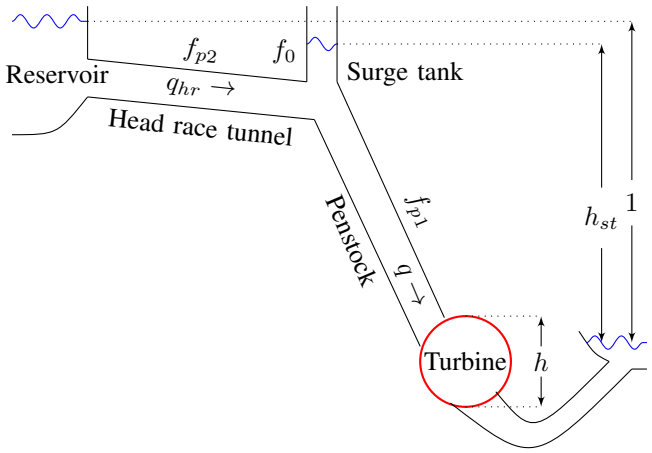

Fig. 3: Waterway layout

2) Outer Controller - Reactive Power Control:

$$\begin{aligned} \frac{d}{dt}N_{c,q} &= k_{Qi}\left(Q_g^* - Q_g\right) \\ i_{g,q}^* &= k_{Qp}\left(Q_g^* - Q_g\right) + N_{c,q} \end{aligned} \tag{3}$$

3) Inner Controller:

$$\begin{aligned} \frac{d}{dt}M_{c,d} &= k_{ii,c}\left(i_{g,d}^* - i_{g,d}\right) \\ v_{c,d}^* &= v_{g,d} - \omega_g l_f i_{g,q} + k_{ip,c}\left(i_{g,d}^* - i_{g,d}\right) + M_{c,d} \\ \frac{d}{dt}M_{c,q} &= k_{ii,c}\left(i_{g,q}^* - i_{g,q}\right) \\ v_{c,q}^* &= v_{g,q} + \omega_g l_f i_{g,d} + k_{ip,c}\left(i_{g,q}^* - i_{g,q}\right) + M_{c,q} \end{aligned} \tag{4}$$

4) Converter Model:

$$\begin{aligned} \frac{d}{dt}v_{c,d} &= \frac{1}{T_{r,c}}\left(v_{c,d}^* - v_{c,d}\right) \\ \frac{d}{dt}v_{c,q} &= \frac{1}{T_{r,c}}\left(v_{c,q}^* - v_{c,q}\right) \end{aligned} \tag{5}$$

5) Filter:

$$\begin{aligned} \frac{d}{dt}i_{g,d} &= \frac{\omega_0}{l_f}\left(v_{c,d} - v_{g,d} - r_f i_{g,d} + \omega_{pll} l_f i_{g,q}\right) \\ \frac{d}{dt}i_{g,q} &= \frac{\omega_0}{l_f}\left(v_{c,q} - v_{g,q} - r_f i_{g,q} - \omega_{pll} l_f i_{g,d}\right) \end{aligned} \tag{6}$$

6) Power Calculation:

$$\begin{aligned} P_g &= v_{g,d} i_{g,d} + v_{g,q} i_{g,q} \\ Q_g &= -v_{g,d} i_{g,q} + v_{g,q} i_{g,d} \end{aligned} \tag{7}$$

7) Dc-link Capacitor Voltage:

$$\begin{aligned} \frac{d}{dt}v_{dc} &= \frac{1}{c}\left(i_{dc,sg} - i_{dc,c}\right) \\ &= \frac{1}{c v_{dc}}\left(P_{sg} - \left(v_{c,d} i_{g,d} + v_{c,q} i_{g,q}\right)\right) \end{aligned} \tag{8}$$

C. Phase-Locked Loop

The phase-locked loop (PLL) in Figure 7 attempts to align the d-axis voltage of the converter $v_{g,d}$ with the voltage at PCC by estimating the PCC voltage phase angle and grid frequency. The PLL model (9) uses a PI controller to control $v_{g,q}$ to zero to achieve this. The SO criteria are obtained to find the PLL controller parameters. The relationship between the converter dq-reference frame and the synchronous reference frame of the grid is given in (10) [18].

$$\begin{aligned} \frac{d}{dt}\theta_{p,pll} &= k_{p,pll}\left(-v_{gRe}\sin\theta_{p,pll} + v_{gIm}\cos\theta_{p,pll}\right) \\ &\quad + x_{pll} \\ \frac{d}{dt}x_{pll} &= k_{i,pll}\left(-v_{gRe}\sin\theta_{p,pll} + v_{gIm}\cos\theta_{p,pll}\right) \\ \omega_{pll} &= \frac{\Delta\omega_{pll}}{\omega_0} + \omega_s \end{aligned} \tag{9}$$

$$\begin{bmatrix} d \\ q \end{bmatrix} = \begin{bmatrix} \cos\theta_{p,pll} & \sin\theta_{p,pll} \\ -\sin\theta_{p,pll} & \cos\theta_{p,pll} \end{bmatrix} \begin{bmatrix} Re \\ Im \end{bmatrix} \tag{10}$$

D. Synchronous Generator

The VSHP-model utilize a sixth-order synchronous generator model as presented in [19]. Since the reactances are dependent on the rotational speed, they cannot be assumed to be constant in a VSHP. The reactances are therefore assumed to be proportional to the rotational speed ω such that $X_x = (\omega_s + \Delta\omega) L_x$.

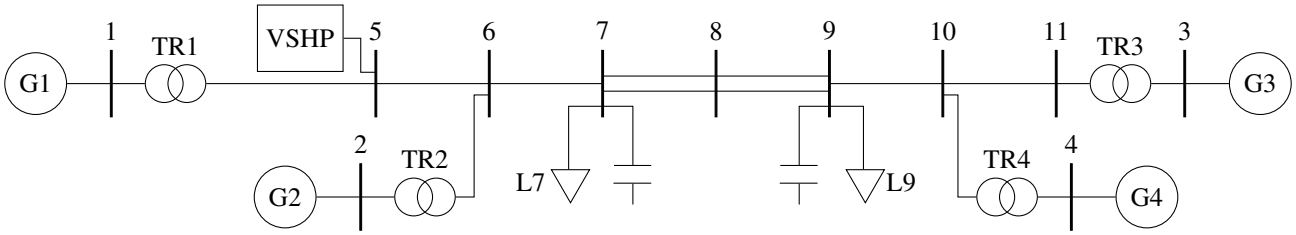

Fig. 4: Kundur Two-area system

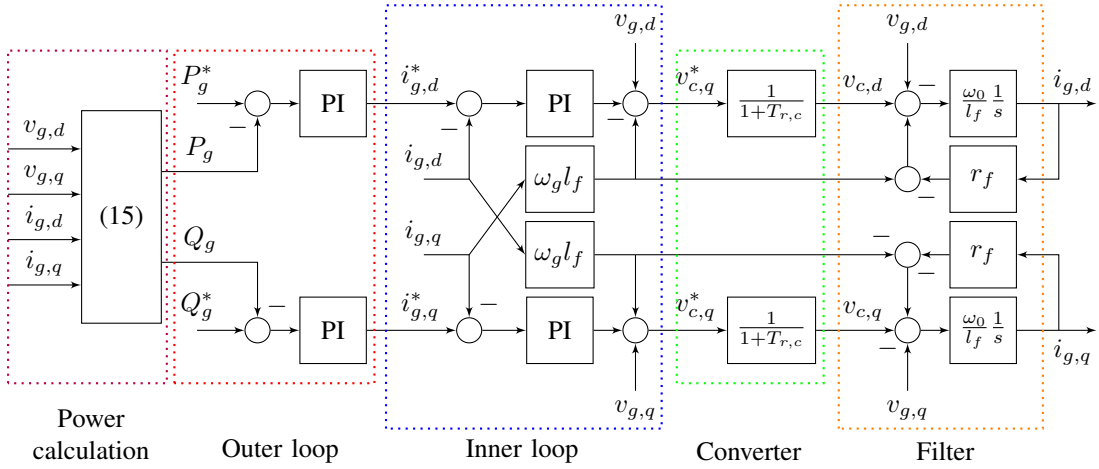

Fig. 5: Grid converter

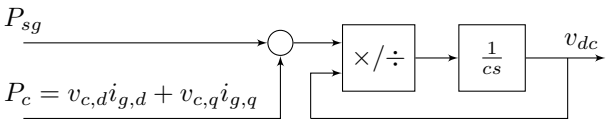

Fig. 6: DC-circuit

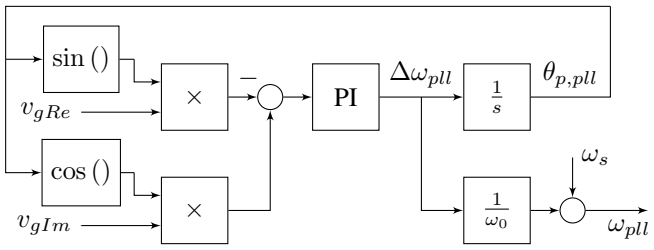

Fig. 7: PLL

The generator current is obtained from the voltage difference between the internal sub-transient generator voltage and converter voltage over the generator impedance:

$$
\begin{aligned}
i_{sg,d} &= \mathrm{Im}\left(\frac{\left(E_q^{''} - v_{c,q}\right) + j\left(E_d^{''} - v_{c,d}\right)}{R_a + j\omega X_d^{''}}\right) \\
i_{sg,q} &= \mathrm{Re}\left(\frac{\left(E_q^{''} - v_{c,q}\right) + j\left(E_d^{''} - v_{c,d}\right)}{R_a + j\omega X_d^{''}}\right)
\end{aligned}
\tag{11}
$$

E. Synchronous Generator Converter

The synchronous generator converter, Figure 8, controls the dc-link voltage v_{dc} by controlling the q-axis current $i_{sg,q}$ in the outer controller (12). In addition to a PI-controller on the dc-voltage error $v_{dc}^* - v_{dc}$, there is a forward coupling on the grid converter output power P_g to increase the precision and speed of the controller. The d-axis current reference $i_{sg,d}$ is set to zero.

The inner controller (13) consist of two PI current controllers with deviation in respectively d-axis current $i_{sg,d}^* - i_{sg,d}$ and q-axix current $i_{sg,q}^* - i_{sg,q}$ as input.

The PI inner and outer controller parameters are calculated by respectively the MO and SO criterion, assuming a switching frequency of 4 kHz.

1) Outer controller:

$$
\begin{aligned}
\frac{d}{dt}N_{sg,q} &= k_{dc,p}\left(v_{dc}^* - v_{dc}\right) \\
i_{sg,q}^* &= k_{dc,i}\left(v_{dc}^* - v_{dc}\right) + N_{sg,q} + P_g \\
i_{sg,d}^* &= 0
\end{aligned}
\tag{12}
$$

2) Inner Controller:

$$
\begin{aligned}
\frac{d}{dt}M_{sg,d} &= k_{ii,sg}\left(i_{sg,d}^* - i_{sg,d}\right) \\
v_{sg,d}^* &= k_{ip,sg}\left(i_{sg,d}^* - i_{sg,d}\right) - \omega L_q^{''} i_{sg,q} + M_d \\
\frac{d}{dt}M_{sg,q} &= k_{ii,sg}\left(i_{sg,q}^* - i_{sg,q}\right) \\
v_{sg,q}^* &= k_{ip,sg}\left(i_{sg,q}^* - i_{sg,q}\right) + \omega L_d^{''} i_{sg,d} + M_q
\end{aligned}
\tag{13}
$$

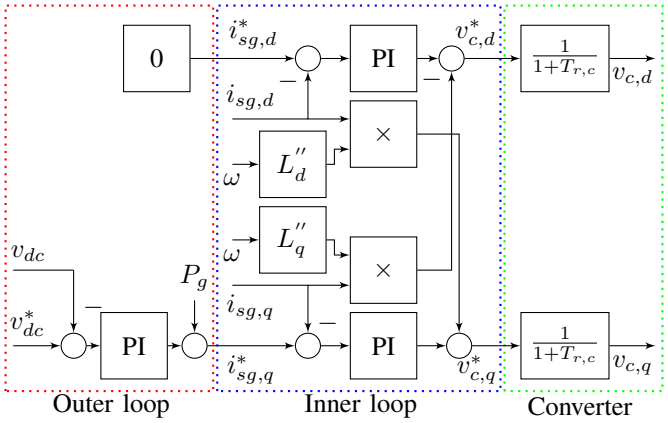

Fig. 8: SG converter

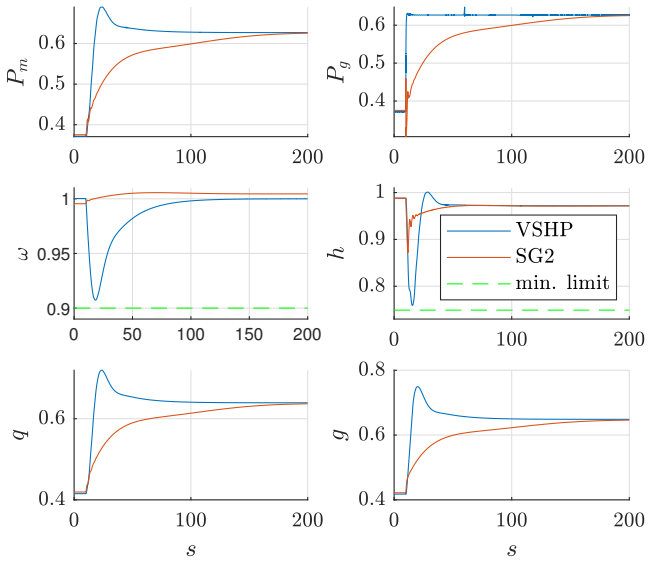

Fig. 9: Step response when power is increased

3) Converter Model:

$$\begin{aligned} \frac{d}{dt}v_{sg,d} &= \frac{1}{T_{r,sg}}\left(v^*_{sg,d} - v_{sg,d}\right) \\ \frac{d}{dt}v_{sg,q} &= \frac{1}{T_{r,sg}}\left(v^*_{sg,q} - v_{sg,q}\right) \end{aligned} \tag{14}$$

4) Power Calculation:

$$\begin{aligned} P_{sg} &= v_{sg,d}i_{sg,d} + v_{sg,q}i_{sg,q} \\ Q_{sg} &= -v_{sg,d}i_{sg,q} + v_{sg,q}i_{sg,d} \\ P_{dc} &= v_{dc}i_{dc,sg} = P_{sg} \end{aligned} \tag{15}$$

IV. Dynamic Analysis

The step responses of a VSHP and a conventional hydropower plant are compared in Figures 9 and 10, for, respectively, increase and reduction in power. The Euler turbine model is used for both types of hydropower plants, however, the governor differs; the VSHP utilizes a PID-controller without permanent droop, the conventional utilizes a droop controller. For the conventional hydropower plant, the step response is applied by a step in reference speed at the governor

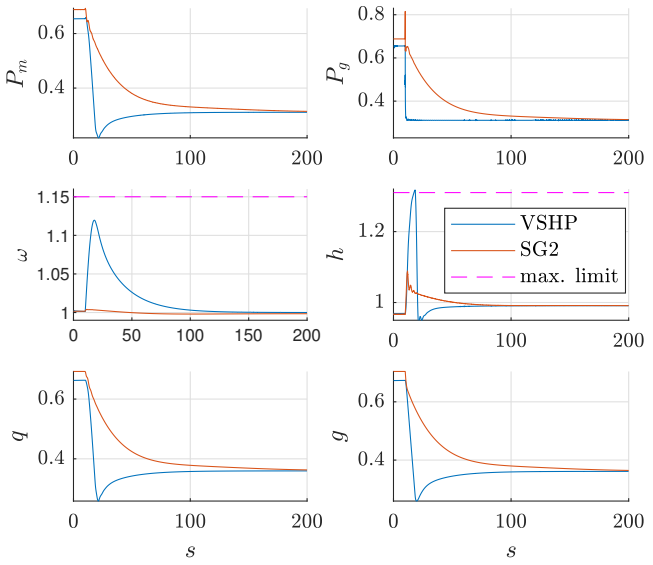

Fig. 10: Step response when power is decreased

input. The VSHP has one more degree of freedom since both the governor reference speed and the grid converter power reference affect the power produced by the turbine. However, a change in the governor reference speed will not cause the output power to the grid to change, only the rotational speed of the turbine. Therefore, the step response of the VSHP is applied to the grid converter power reference.

For fully utilizing the potential of ancillary services from a VSHP, the power delivery to the grid needs to be as flexible and quickly as possible. The power control of the VSHP grid converter allows the power output to the grid P_g to follow the step response in power reference almost perfectly.

However, the turbine power P_m will not be able to react as quickly, due to the governor and servo time constants. The deviation between the grid converter power P_g and the turbine power P_m will cause a deviation in rotational speed ω, approximately equal to the integration of the difference $P_m - P_g$. Next, the governor reacts to regain the reference rotational speed, causing the guide vane opening g and turbine water flow q to change. This causes changes in surge tank head h_{st}, headrace tunnel flow q_{hr}, turbine head h and turbine power P_m. The maximum size of the grid converter power step is thereby limited by the limits of the variables in the waterway, governor, turbine, SG and SG converter:

- maximum allowed rotational speed of the turbine/SG
- minimum rotational speed to regain the reference rotational speed, as pointed out in [10]
- minimum and maximum limits of the governor
- rate limit of the governor
- surge tank head limits
- current limits of the SG converter and the SG

As Figures 9 and 10 show, the fast change in output power of the VSHP causes larger peaks in mechanical power P_m, rotational speed ω, pressure (head) high h, flow q and guide vane opening g compared to a conventional hydropower plant. These variables must be within the limits given above. Increased wear and tear on the guide vane servo due to

additional operation and on the waterway due to more water hammering and mass oscillations must also be considered when designing the control system.

Although the power reference step in the two figures is the same, larger deviations in h, g, q and ω are observed when the power is reduced, compared to the case with an increase in power. From the Euler turbine equations, we see that the turbine mechanical power P_m decreases slower from an initial high power operational point when ω is increasing than P_m increases for an initial low operation point when ω increases. This causes a larger deviation in ω, faster operation of the guide vane opening g and hence larger overshoot in the head h and the flow q.

V. Participation Factor Based Interaction Analysis

A participation factor-based interaction mode method proposed in [20] is used to investigate the interactions between the subsystems. An interaction mode is defined as a mode with participation from more than one subsystem and proves a dynamic interaction between the subsystems [18].

The participation factor p_{ki} of state variable x_k in mode i is defined in [15] as

$$p_{ki} = \phi_{ki}\psi_{ki} \tag{16}$$

where ϕ and ψ are respectively the right and left eigenvector. The parameter $\eta_{\alpha i}$ is defined in [20] as a measure for the overall participation for each subsystem α in mode i.

$$\eta_{\alpha i} = \frac{||p_{\alpha i||}}{||p_i||} \tag{17}$$

where $||\cdot||$ denotes the L_1-norm. While the participation factor p_{ki} measures the participation of a state variable in a mode, $\eta_{\alpha i}$ calculates the degree of participation of a group for state variable, a subsystem, in a mode.

The VSHP system is divided into 12 subsystems, as presented on the y-axis in Figure 11. The modes on the x-axis are sorted according to the participation in each subsystem. The colours show the magnitude of $\eta_{\alpha i}$ for each subsystem and mode. The modes only participating in generators G1-G4 are not presented in the figure.

The participation factor-based interaction analysis presented in Figure 11 shows that the system can be divided into two parts, where no modes are interacting in both these parts. The division is between the two converters in the VSHP. The turbine side of the DC-link includes VSHP waterway, VSHP turbine, VSHP governor, VSHP generator, SG converter and DC-link while the grid side of the DC-link includes the subsystems that are interfering with the other generators in the grid; the grid converter and the PLL.

The reason why there are no modes between the two parts can be found by investigating the variables between the subsystems in Figure 1. The turbine side of the DC-link will be affected by a perturbation on the grid side of the turbine since this will cause the DC-voltage and thereby the power of the SG converter to change. A perturbation on the turbine side of the DC-link will also cause the DC-link voltage to change; however, the grid converter control is not influenced by the DC-link voltage, see Figure 5. Since the two parts do not influence each other, there will be no modes between the two parts.

A more detailed model of the grid converter may consider the DC-link voltage, for instance when calculating the PWM modulation. However, this is only compensating for a deviation in DC-voltage such that the converter output voltage follows the reference voltage. Therefore, this will, in practice, not result in any new coupling between the two parts.

We believe that the proposed control system in this paper is perfectly suited for VI control of the grid converter for two reasons. Firstly, the control system has very good performance from a grid perspective since no modes are interacting between the VSHP turbine, waterway and generator and the rest of the grid. The output power of the VSHP can, therefore, be controlled directly by the grid converter with great flexibility without considering small signal stability issues in the turbine side of the DC-link. This makes the design of the VI controller easier than alternative control layouts; i.e. if the governor is controlled by the grid frequency as in a conventional hydropower plant or if the SG converter is controlled by the grid frequency and the governor controls the turbine rotational speed. Secondly, the control system makes it possible to use the rotational energy of the turbine and the generator as energy storage by allowing the turbine rotational speed to deviate from its nominal value. The VI control of the grid converter utilizes this energy storage to deliver faster power response to the grid. However, there are still limitations due to the maximum speed of the governor, the limits of the turbine rotational speed range and turbine head and water hammering in the penstock that affect the VSHP output power control ability. VI will be implemented and tested in further works to verify this assumption.

VI. Conclusion

A detailed model of a VSHP plant, including hydraulic system models and converter models, has been developed and presented in this paper. The model is tested for the purpose of utilizing the VSHP for ancillary services and to explore the limitations given by the hydraulic system. The results are compared with a conventional hydropower plant. A key finding is that in variable speed operation the gradients and peaks in guide vane opening, flow and head tend to become more excited due to the larger deviations in turbine rotational speed.

Extra awareness when designing the control system is therefore needed to keep the hydraulic system variables, such as the surge tank head, within their limits.

The participation factor-based interaction analysis shows that the VSHP-system can be divided into two parts where there is no mode interacting in both parts. The turbine side of the DC-link will be affected by a perturbation on the grid side of the DC-link; however, there is no coupling the other way since the grid converter control is not influenced by the DC-link voltage. The result is that there will be no modes

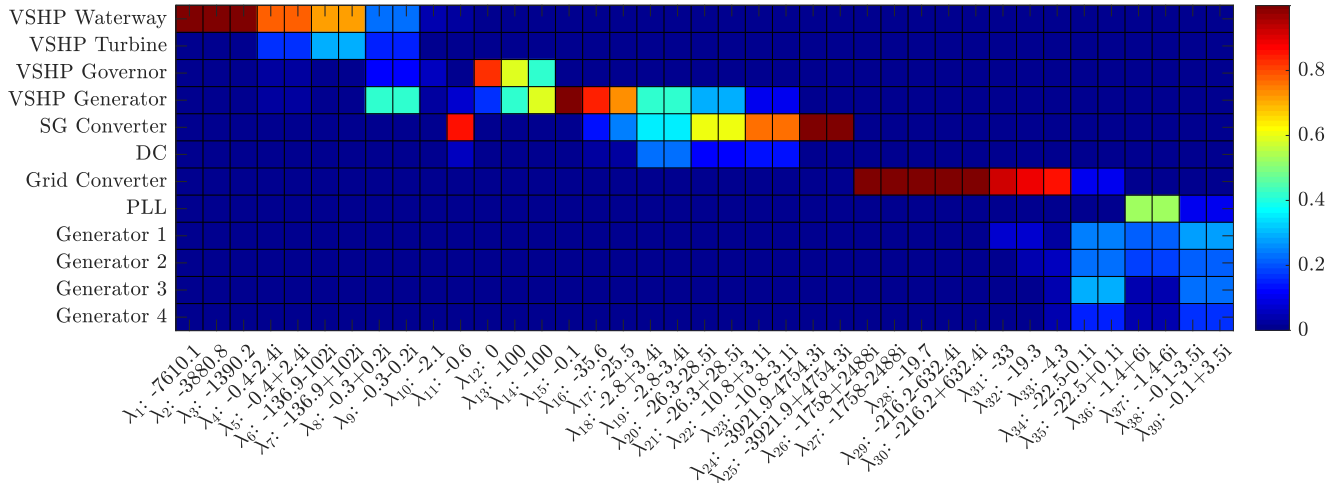

Fig. 11: Participation factor-based interaction analysis

between the hydraulic system of the VSHP and the rest of the grid, and, from a small signal perspective, that the modes of the hydraulic system will not need to be considered when tuning the grid converter.

The possibility for utilizing the rotational energy in the turbine and generator and controlling the output power without causing small-signal instability in the hydraulic system makes VSHP very suitable for VI control. However, the limitations in the hydraulic system must be fulfilled. For this reason, more advanced control systems considering such limits, such as model predictive control, might be favourable to optimize the ancillary services given by the VSHP.

Appendix A
Parameters, Set-points and Variables

The model parameters and set-points are given in Table I while the variables are given in Table II.

References

[1] M. Valavi and A. Nysveen, "Variable-speed operation of hydropower plants: Past, present, and future," in *Electrical Machines (ICEM), 2016 XXII International Conference on*. IEEE, 2016, pp. 640–646.

[2] Y. Pannatier, B. Kawkabani, C. Nicolet, J.-J. Simond, A. Schwery, and P. Allenbach, "Investigation of control strategies for variable-speed pump-turbine units by using a simplified model of the converters," *IEEE Transactions on Industrial Electronics*, vol. 57, no. 9, pp. 3039–3049, 2010.

[3] M. Mohanpurkar, A. Ouroua, R. Hovsapian, Y. Luo, M. Singh, E. Muljadi, V. Gevorgian, and P. Donalek, "Real-time co-simulation of adjustable-speed pumped storage hydro for transient stability analysis," *Electric Power Systems Research*, vol. 154, pp. 276–286, 2018.

[4] A. Ansel and B. Robyns, "Modelling and simulation of an autonomous variable speed micro hydropower station," *Mathematics and computers in simulation*, vol. 71, no. 4-6, pp. 320–332, 2006.

[5] S. Breban, A. Ansel, M. Nasser, B. Robyns, and M. M. Radulescu, "Experimental results on a variable-speed small hydro power station feeding isolated loads or connected to power grid," in *Electrical Machines and Power Electronics, 2007. ACEMP'07. International Aegean Conference on*. IEEE, 2007, pp. 760–765.

[6] E. Muljadi, M. Singh, V. Gevorgian, M. Mohanpurkar, R. Hovsapian, and V. Koritarov, "Dynamic modeling of adjustable-speed pumped storage hydropower plant," in *Power & Energy Society General Meeting, 2015 IEEE*. IEEE, 2015, pp. 1–5.

[7] T. Mercier, M. Olivier, and E. Dejaeger, "Operation ranges and dynamic capabilities of variable-speed pumped-storage hydropower," in *Journal of Physics: Conference Series*, vol. 813, no. 1. IOP Publishing, 2017, p. 012004.

[8] W. Yang and J. Yang, "Advantage of variable-speed pumped storage plants for mitigating wind power variations: Integrated modelling and performance assessment," *Applied Energy*, vol. 237, pp. 720–732, 2019.

[9] A. Béguin, C. Nicolet, J. Hell, and C. Moreira, "Assessment of power step performances of variable speed pump-turbine unit by means of hydro-electrical system simulation," in *Journal of Physics: Conference Series*, vol. 813, no. 1. IOP Publishing, 2017, p. 012001.

[10] T. I. Reigstad and K. Uhlen, "Modelling of variable speed hydro power for grid integration studies," *Manuscript submitted for publication*.

[11] D. Borkowski and T. Wegiel, "Small hydropower plant with integrated turbine-generators working at variable speed," *IEEE Transactions on Energy Conversion*, vol. 28, no. 2, pp. 452–459, 2013.

[12] J. Marquez, M. Molina, and J. Pacas, "Dynamic modeling, simulation and control design of an advanced micro-hydro power plant for distributed generation applications," *International journal of hydrogen energy*, vol. 35, no. 11, pp. 5772–5777, 2010.

[13] F. Demello, R. Koessler, J. Agee, P. Anderson, J. Doudna, J. Fish, P. Hamm, P. Kundur, D. Lee, G. Rogers *et al.*, "Hydraulic-turbine and turbine control-models for system dynamic studies," *IEEE Transactions on Power Systems*, vol. 7, no. 1, pp. 167–179, 1992.

[14] T. K. Nielsen, "Simulation model for francis and reversible pump turbines," *International Journal of Fluid Machinery and Systems*, vol. 8, no. 3, pp. 169–182, 2015.

[15] P. Kundur, N. J. Balu, and M. G. Lauby, *Power system stability and control*. McGraw-hill New York, 1994, vol. 7.

[16] C. Bajracharya, M. Molinas, J. A. Suul, T. M. Undeland *et al.*, "Understanding of tuning techniques of converter controllers for vsc-hvdc," in *Nordic Workshop on Power and Industrial Electronics (NORPIE/2008), June 9-11, 2008, Espoo, Finland*. Helsinki University of Technology, 2008.

[17] S. D'Arco, J. A. Suul, and O. B. Fosso, "Control system tuning and stability analysis of virtual synchronous machines," in *2013 IEEE Energy Conversion Congress and Exposition*. IEEE, 2013, pp. 2664–2671.

[18] A. G. Endegnanew, "Stability analysis of high voltage hybrid ac/dc power systems," 2017.

[19] J. Machowski, J. Bialek, J. R. Bumby, and J. Bumby, *Power system dynamics and stability*. John Wiley & Sons, 1997.

[20] J. Beerten, S. D'Arco, and J. A. Suul, "Identification and small-signal analysis of interaction modes in vsc mtdc systems," *IEEE Transactions on Power Delivery*, vol. 31, no. 2, pp. 888–897, 2016.

TABLE I: Parameters and set-points

Parameter	Value
Waterway	
Rated water flow Q_R, $[m^3/s]$	170
Rated height H_R, $[m]$	425
Penstock:	
Water starting time T_w, $[s]$	1.211
Water traveling time T_e, $[s]$	0.126
Characteristic impedance Z_0	9.61
Friction factor f_{p1}, $[s^4/m^5]$	0.049
Surge tank:	
Friction factor f_{p0}, $[s^4/m^5]$	0.036
Storage constant C_s	0.099
Head race tunnel:	
Water starting time T_{w2}, $[s]$	4.34
Friction factor f_{p2}, $[s^4/m^5]$	0.020
Hydraulic Machine	
Turbine constant ψ	0.404
Turbine constant ξ	0.918
Turbine constant α	0.745
Turbine constant σ	0.015
Rated water flow Q_{Rt}, $[m^3/s]$	144
Rated height H_{Rt}, $[m]$	425
Governor conventional hydropower	
Governor time constant T_r, $[s]$	4.00
Servo time constant T_g, $[s]$	0.50
Temporary droop r	0.40
Permanent droop R	0.05

Parameter	Value
Governor VSHP	
Rotational speed reference ω^*, pu	1.00
Governor proportional gain $k_{g,p}$	3.00
Governor integration gain $k_{g,i}$	0.100
Governor derivation gain $k_{g,d}$	1.000
Rate limit	+/-0.05
Servo time constant T_G, $[s]$	0.500
Synchronous generator	
Inertia constant H, $[s]$	6.5
Damping constant D	0
Stator resistance R_a, pu	2.5e-3
Transient time constants:	
$T^{'}_{d0}$, $[s]$	8
$T^{'}_{q0}$, $[s]$	0.4
Sub-transient time constants:	
$T^{''}_{d0}$, $[s]$	0.03
$T^{''}_{q0}$, $[s]$	0.05
Synchronous reactances:	
X_d, pu	1.8
X_q, pu	1.7
Transient reactances:	
$X^{'}_{d}$, pu	0.3
$X^{'}_{q}$, pu	0.55
Sub-transient reactances:	
$X^{''}_{d}$, pu	0.25
$X^{''}_{q}$, pu	0.25

Parameter	Value
SG converter	
Switching time delay $T_{r,sg}$, $[ms]$	0.25
Inner controller:	
Proportional gain $k_{ip,sg}$	0.3
Integral gain $k_{ii,sg}$	20
Outer controller:	
Dc-voltage reference v^*_{dc}	1.00
Proportional gain $k_{dc,p}$	0.64
Integral gain $k_{dc,i}$	0.082
Grid converter	
Inner controller:	
Proportional gain $k_{ip,c}$	0.509
Integral gain $k_{ii,c}$	10
Outer controller:	
Proportional gain k_{Pp},k_{Qp}	21.2
Integral gain k_{Pi},,k_{Qi}	94.3
Converter and filter:	
Switching time delay $T_{r,c}$, $[ms]$	1.00
Filter resistance r_f, pu	0.01
Filter impedance l_f, pu	0.16
PLL:	
Proportional gain $k_{p,pll}$	2.26
Integral gain $k_{i,pll}$	34.3
Base grid frequency ω_0, rad/s	$2\pi f$
Dc-link:	
Capacitance c, pu	0.02

TABLE II: Variables

Variable	Symbol
Waterway	
Surge tank head	h_{st}
Head race tunnel flow	q_{hr}
Hydraulic Machine	
Turbine head	h
Turbine water flow	q
Mechanical torque	T_m
Mechanical power	P_m
Turbine efficiency	η_h
Turbine head	h_t
Turbine flow	q_t
Opening degree of turbine	κ
Governor	
Guide vane opening reference	g^*
Guide vane opening	g

Variable	Symbol
Synchronous generator	
Rotor angle	δ
Rotor speed deviation	$\Delta\omega$
Transient voltages	$E^{'}_{d}$, $E^{'}_{q}$
Sub-transient voltages	$E^{''}_{d}$, $E^{''}_{q}$
Field excitation voltage	E_{fd}
Stator currents	$i_{sg,d}$, $i_{sg,q}$
Stator voltage	$v_{sg,d}$, $v_{sg,q}$
Electrical power	P_e
SG converter	
Stator current references	$i^*_{sg,d}$, $i^*_{sg,q}$
Stator voltage references	$v^*_{sg,d}$, $v^*_{sg,q}$
Active/reactive power	P_{sg}, Q_{sg}
Dc-link power	P_{dc}
Dc-link voltage	v_{dc}

Variable	Symbol
Grid converter	
Grid currents	$i_{g,d}$, $i_{g,q}$
Grid current references	$i^*_{g,d}$, $i^*_{g,q}$
Converter voltages	$v_{c,d}$, $v_{c,q}$
Converter voltage references	$v^*_{c,d}$, $v^*_{c,q}$
Grid voltage	$v_{g,d}$, $v_{g,q}$
Active/reactive power	P_g, Q_g
Active/reactive power ref.	P^*_g, Q^*_g
PLL	
Estimated PCC voltage angle	$\theta_{p,pll}$
Speed deviation of converter control	$\Delta\omega_{pll}$
Reference machine speed	ω_s
Real part of PCC voltage	v_{gRe}
Imaginary part of PCC voltage	v_{gIm}

Tor Inge Reigstad received his M.Sc degree from Department of Electric Power Engineering at the Norwegian University of Science and Technology (NTNU), Trondheim, Norway, in 2007. He previously work with Siemens AS and SINTEF Energy Research, both Trondheim, until he started his PhD studies within grid integration of variable speed hydropower in 2018. His current research interests are principally related to the analysis and control of power electronic converters in onshore and offshore grids.

Kjetil Uhlen is a professor in Power Systems at the Norwegian University of Science and Technology (NTNU), Trondheim, and a Special Adviser at STATNETT (the Norwegian TSO). He has a Master's degree (1986) and PhD degree (1994) in control engineering. His main areas of work include research and education within control and operation of power systems, grid integration of renewable energy and power system dynamics.